QUASI-LUMPED DESIGN OF UWB BPF USING SUSPENDED STRIPLINE

X.-J. Liao

Graduate Institute of Communications Engineering
National Changhua University of Education
2, Shih-Ta Rd., Changhua City 50074, Taiwan

M.-H. Ho

Department of Electronic Engineering
Graduate Institute of Communications Engineering
National Changhua University of Education
2, Shih-Ta Rd., Changhua City 50074, Taiwan

W.-H. Hsu, W.-Q. Xu, and L.-J. Lin

Universal Microwave Technology, Inc.
1, Gongjian Road., Cidu District, Keelung City 20647, Taiwan

Abstract—We propose a novel UWB bandpass filter (BPF) design using the suspended stripline (SSL). The filter composes of a low-pass and a high-pass circuit, both implemented by SSL structures. A notch response structure might be implemented to the filter by embedding a resonant slotline. The quasi-lumped elements circuit models were developed to analyze these circuits' performance. Experiments were conducted, and good agreements were observed between the measurements and simulations.

1. INTRODUCTION

Various transmission line structures have been applied to build the UWB filters [1–6]. In [1], the multimode resonators combining with parallel microstrips were used to construct the filters. The utilization of the parallel-coupled microstrips together with the open stubs achieved the wide-band performance with providing extra transmission zeros

---

Corresponding author: M.-H. Ho (ho@cc.ncue.edu.tw).

in the stopband [2]. Recently, the SSL implemented the filter's structure to accomplish the wide band requirement with very low insertion losses and good immunity of radiation noise [3]. The compact fork-form resonators were applied to a UWB filter which exhibited two attenuation poles near both passband edges [4]. It possessed lower insertion losses compared with the traditional parallel-coupled lines filters. In [5], wideband response circular slots were embedded in the ground plane for a UWB filter design, which achieved extremely low in-band insertion losses. In [6], they applied the SSL to build the bandstop filter. Compared with microstrips and the other planar structures (e.g., CPW, slotline, and stripline) used in the filter designs, the SSL structure inherited the advantages of high frequency operation, low radiation and dielectric losses, and better electromagnetic immunity and susceptibility. Besides, the usage of the substrate's two sides diversified the circuit design and might reduce the circuit size. Furthermore, the side walls of the shielding metal serving as the circuit's ground benefited the multilayered circuits in eliminating the ground layers which normally occupied a few.

In this research, we present a novel UWB BPF of SSL structure. The RT/Duroid 5880 substrate with a thickness of 0.254-mm and a dielectric constant of $\epsilon_r = 2.2$ was selected to bear the filter's metal patterns. The substrate was suspended horizontally in the middle of the metal channel having dimensions of 5-mm in width and 4.254-mm in height. The UWB filter with its passband conforming to unlicensed use of frequency band in 3.1–10.6 GHz was built from combining a low-pass and a high-pass filter of SSL structure. The low-pass and the high-pass circuit were designed upon a 7th order elliptical function responses. Alternatively, a notch-response slotline might be embedded in the SSL's signal strip to avoid the WLAN's signal interference in the range 5.17–5.875 GHz. Equivalent lumped-elements circuit models were developed to analyze each individual circuit's performance. The values of the lumped elements were obtained upon the quasi-lumped approach [7] or were extracted from simulated S-parameter data. The full-wave simulation (HFSS) was further used to validate the circuit models during the design. Experiment was conducted to verify the circuit design. Good agreements were observed between the simulated and measured data.

2. UWB BPF DESIGN

2.1. Low-Pass Circuit Design

Figure 1 shows the top and bottom layout of the SSL low-pass filter structure with the equivalent LC circuit model given in Fig. 2. Note
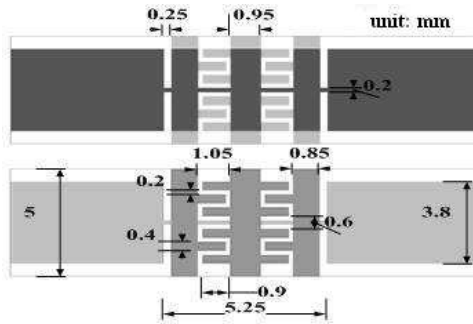
Figure 1. The top and bottom layout of the SSL low-pass circuit (dimension in mm).
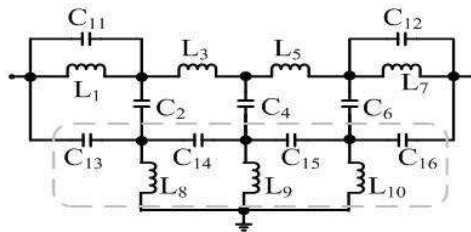
Figure 2. The equivalent circuit model of the circuit in Fig. 1 ($L_1 = L_7 = 0.650$ nH, $L_3 = L_5 = 1.21$ nH, $L_8 = L_{10} = 0.172$ nH, $L_9 = 0.554$ nH, $C_2 = C_6 = 0.36$ pF, $C_4 = 0.52$ pF, $C_{13} = C_{16} = 0.08$ pF, $C_{14} = C_{15} = 0.17$ pF, and $C_{11} = C_{12} = 0.06$ pF).
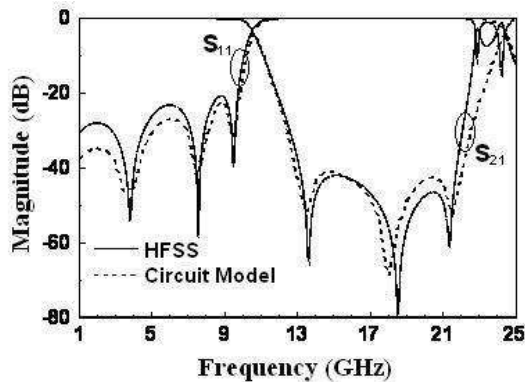
Figure 3. The circuit model's frequency responses for the low-pass circuit.

here, the series capacitance, C_{11} and C_{12}, represent the proximity couplings of the I/O strips and their neighboring ones on the same side. In the dashed box, the capacitances C_{14} and C_{15} represent the couplings of the interdigital structures in Fig. 1. The capacitances C_{13} and C_{16} stand for the couplings between each of the I/O strips and the nearby ones on the opposite side. As shown in Fig. 3, the equivalent LC circuit model, while omitting the effects of those elements in the dashed box, gives an elliptical response having a transmission zero (the second zero) around 18.2 GHz. This transmission zero is dominated by the resonance of the series block consisting of L_1 (L_7) and C_{11} (C_{12}).

When accounting for the effect of dashed box circuit, those representing the effect of the inter-digitally coupled structure can improve the filter's signal selectivity from the zero (the first zero in Fig. 3) which is much closer to the band edge than the one of 18.2 GHz. The circuit enclosed by the dashed box actually arises two extra transmission zeros located at around 13.2 GHz and 22.01 GHz. The first zero increases significantly the roll-off slope of the band edge, results in a better signal selectivity. And it together with the rest zeros improves the stopband performance by increasing the stopband's signal rejection. The calculated stopband bandwidth (BW) was 11.32 GHz under the 30-dB out-of-band signal rejection level.

2.2. High-Pass Circuit Design

The structure of the high-pass circuit is proposed in Fig. 4 and its equivalent lumped-elements circuit model is given in Fig. 5. The series capacitances represent the coupling between the top and the bottom
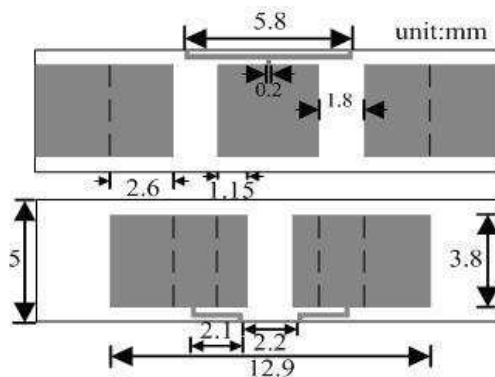
Figure 4. The top and bottom layout of the SSL high-pass circuit (dimension in mm).
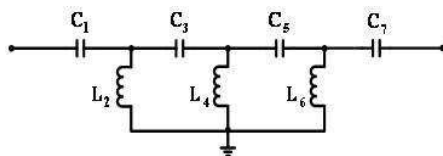
Figure 5. The equivalent circuit model of the circuit in Fig. 4 ($C_1 = C_7 = 1.1204\,\mathrm{pF}$, $C_3 = C_5 = 0.5108\,\mathrm{pF}$, $L_2 = L_6 = 1.5431\,\mathrm{nH}$, $L_4 = 1.3869\,\mathrm{nH}$).
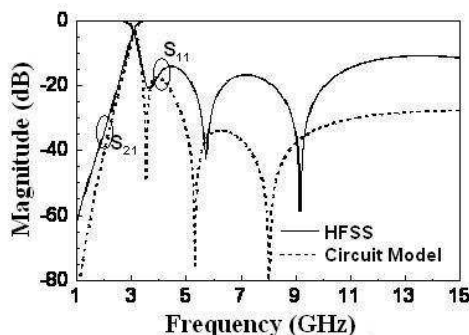
Figure 6. The circuit model's frequency response (compared with HFSS simulation) for the high-pass circuit.

patches, and the shunt inductances denote the current effects on the narrow strips branching of the patches to the side wall ground. This circuit model was initially verified by the HFSS simulation. In Fig. 6, we show the circuit model's frequency response, which is compared with the one obtained by HFSS. The achieved 3-dB point (joint of the S_{11} and S_{21}) is located at 3.09 GHz.

3. SAMPLE UWB BPF RESULTS

The proposed UWB BPF was built from cascading the above mentioned low-pass and high-pass circuit. In Fig. 7, we give the measured and simulated frequency response, and the inset is the measured group delays. Note here, the simulation in Fig. 7 is obtained by HFSS. It is observed that the agreement is quite well between the simulation and measurement. The group delays vary between 0.4–0.5 ns in the range of 3.5–10.6 GHz. The in-band insertion losses are within the range 0.306–0.82 dB and the measured upper stopband BW is 10.88 GHz with the insertion losses greater than 30 dB.

Figure 8 shows the structure of the notch-response slotline embedded in the SSL's signal strip. It has a band rejection function due to the slotline's resonance. This band-rejection slotline can be equivalent to a series block of an L and a C in a parallel connection. The L represents the current effect concentrating on the protruded metal strips and the C accounts for the coupling between the strips. The resonant frequency is evaluated by $1/2\pi\sqrt{LC}$ with $L = 0.372\,\mathrm{nH}$
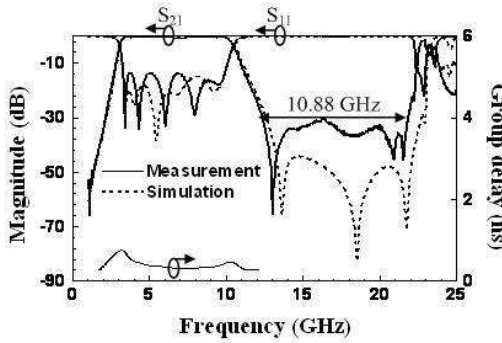
Figure 7. The measured and simulated frequency responses measured group delay (inset) for the UWB BPF.
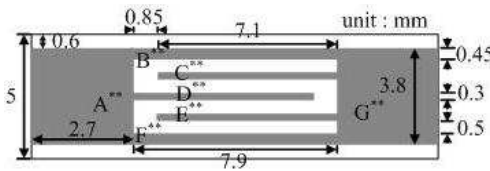
Figure 8. The embedded notch-response slotline structure.
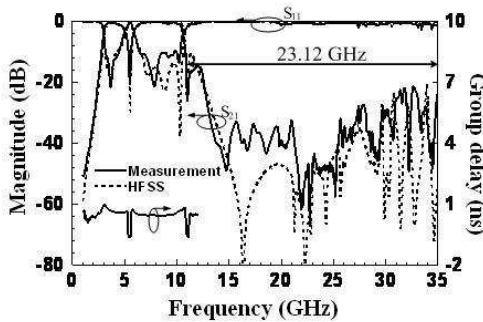
Figure 9. The measured and simulated frequency responses and measured group delay (inset) for the notch UWB filter.

and $C = 2.234\,\mathrm{pF}$. In Fig. 9, we show the wide-band frequency responses of the measured and the simulated results for the notch UWB filter. The passband is from 3.08 to 10.62 GHz with a band notch covering from 5.15 to 5.875 GHz (3-dB BW). The band-notch response is created by the first resonance (at 5.5 GHz) of the slotline which in addition has other two resonances at 10.9 and 22.5 GHz. The second transmission zero (caused by the second resonance) can be observed by the passband's upper edge in Fig. 9. Also shown in the figure, the LPF's upper spurious passband around 23 GHz observed in Figs. 3 and 7 are successfully suppressed by the third zero of the slotline, results in the band-notch UWB filter a much wider stopband BW. The minimum insertion loss is 0.29 dB and the maximum signal rejection level in the notch is 21.3 dB. As shown in Fig. 9, the upper stopband BW (more than 23.12 GHz) is very wide. The inset in Fig. 9 provides the information of the measured group delays. They vary, in the passband excluding the notch zone and the band edges, from 0.395 to 0.54 ns. And the rapid group delay variation in the notch band and the UWB band edges is caused by the rapid changes in frequency response.

4. CONCLUSION

In this work, the low-pass, high-pass, and band-rejection circuits of SSL structure were presented, and their corresponding lumped-elements circuit models were developed to analyze circuit performance. The sample UWB filter design with or without the notch-response slotline was demonstrated, and its measured and simulated frequency responses were given. The SSL's two-sides design might reduce the filter's size. Experiments were conducted to verify the circuit performance. The proposed quasi-lumped approach should be very helpful in designing the SSL filters of various purposes.

ACKNOWLEDGMENT

REFERENCES

1. Sun, S., W. Menzel, and L. Zhu, "Ultra-wideband (UWB) bandpass filters using multiple-mode resonator," *IEEE Microw. Wireless Compon. Lett.*, Vol. 15, No. 11, 796–798, Nov. 2005.

2. Singh, P. K., S. Basu, and Y.-H. Wang, "Planar ultra-wideband bandpass filter using edge coupled microstrip lines and stepped impedance open stub," *IEEE Microw. Wireless Compon. Lett.*, Vol. 17, No. 9, 649–651, Sept. 2007.

3. Menzel, W., M. S. R. Tito, and L. Zhu, "Low-loss ultra-wideband (UWB) filters using suspended stripline," *Asia-Pacific Microwave Conf. Proc. (APMC'05)*, Vol. 1, 2148–2151, Dec. 2005.

4. Chen, H. and Y. Zhang, "A novel and compact UWB bandpass filter using microstrip fork-form resonators," *Progress In Electromagnetics Research*, PIER 77, 273–280, 2007.

5. Naghshvarian-Jahromi, M. and M. Tayarani, "Miniature planar UWB bandpass filters with circular slots in ground," *Progress In Electromagnetics Research Letters*, Vol. 3, 87–93, 2008.

6. Hsu, W.-H. and M.-H. Ho, "Bandstop filter design using the suspended stripline structure," *Asia-Pacific Microwave Conf. Proc. (APMC'08)*, Vol. A2-06, Dec. 2008.

7. Bahl, I. and P. Bhartia, *Microwave Solid State Circuit Design*, 2nd edition, Vol. 6, John Wiley & Sons, N. J., 2003.